# Pentadienyl–Metal–Phosphine Chemistry. 16.[1] Reaction Chemistry of ($\eta^3$-2,4-Dimethylpentadienyl)Rh($PEt_3$)$_2$ and ($\eta^3$-2,4-Dimethylpentadienyl)Rh($PMe_3$)$_2$

John R. Bleeke* and Andrew J. Donaldson

*Department of Chemistry, Washington University, St. Louis, Missouri 63130*

*Received December 21, 1987*

The reactions of ($\eta^3$-2,4-dimethylpentadienyl)Rh($PEt_3$)$_2$ (**1**) and ($\eta^3$-2,4-dimethylpentadienyl)Rh($PMe_3$)$_2$ (**2**) with $CH_3{}^+O_3SCF_3{}^-$ produce ($\eta^5$-2,4-dimethylpentadienyl)Rh($PEt_3$)$_2$(Me)$^+O_3SCF_3{}^-$ (**3**) and ($\eta^5$-2,4-dimethylpentadienyl)Rh($PMe_3$)$_2$(Me)$^+O_3SCF_3{}^-$ (**4**), respectively. The solid-state structure of **3** has been determined by single-crystal X-ray diffraction. The complex crystallizes in the monoclinic space group $P2_1/c$ with $a$ = 11.310 (2) Å, $b$ = 13.507 (7) Å, $c$ = 18.226 (3) Å, $\beta$ = 95.97 (2)°, $V$ = 2769 (3) Å$^3$, and $Z$ = 4. The coordination geometry of **3** is pseudooctahedral, with C(1), C(3), and C(5) of the 2,4-dimethylpentadienyl ligand and P(1), P(2), and C(8) (methyl carbon) occupying the six coordination sites. One of the phosphine ligands resides under the open "mouth" of the 2,4-dimethylpentadienyl ligand, while the other phosphine and the methyl group occupy the coordination sites under the "edges" of the 2,4-dimethylpentadienyl ligand. Upon heating in solution, the 2,4-dimethylpentadienyl ligand in **3** rotates with respect to the $RhP_2$(Me) framework, exchanging the two phosphines, as well as the two ends of the 2,4-dimethylpentadienyl ligand. The energy of activation ($\Delta G^{\ddagger}$) for this dynamic process, derived from variable-temperature NMR studies, is 17.0 ± 0.7 kcal/mol. Treatment of **3** and **4** with $(Ph_3P)_2N^+Cl^-$ produces ($\eta^3$-2,4-dimethylpentadienyl)Rh($PEt_3$)$_2$(Me)(Cl) (**5**) and ($\eta^3$-2,4-dimethylpentadienyl)Rh($PMe_3$)$_2$(Me)(Cl) (**6**), respectively. Compound **5** crystallizes in the monoclinic space group $P2_1/c$ with $a$ = 12.962 (3) Å, $b$ = 8.236 (2) Å, $c$ = 22.758 (6) Å, $\beta$ = 94.19 (2)°, $V$ = 2423 (2) Å$^3$, and $Z$ = 4. The coordination geometry of **5** is pseudooctahedral with C(1), C(3) (2,4-dimethylpentadienyl group), P(1), P(2), C(8) (methyl carbon), and Cl occupying the six coordination sites. The phosphines are trans to the 2,4-dimethylpentadienyl group, while the methyl and chloro ligands reside trans to one another. The $\eta^3$-2,4-dimethylpentadienyl ligand has a syn geometry and is sickle-shaped. In solution, **5** undergoes a dynamic process involving isomerization of the 2,4-dimethylpentadienyl ligand from $\eta^3$ to $\eta^1$ coordination ($\Delta G^{\ddagger}$ = 13.0 ± 0.5 kcal/mol). Treatment of **5** with 2 equiv of $PMe_3$ produces **6** quantitatively. Treatment of **1** with $HBF_4{\cdot}OEt_2$ yields ($\eta^4$-2,4-dimethylpentadiene)Rh($PEt_3$)$_2{}^+BF_4{}^-$ (**7**), which reacts in situ with benzene and durene to release 2,4-dimethylpentadiene and produce ($\eta^6$-benzene)Rh($PEt_3$)$_2{}^+BF_4{}^-$ (**8**) and ($\eta^6$-durene)Rh($PEt_3$)$_2{}^+BF_4{}^-$ (**9**), respectively. Compound **9** crystallizes in the monoclinic space group $P2_1/n$ with $a$ = 8.349 (2) Å, $b$ = 10.843 (8) Å, $c$ = 29.535 (9) Å, $\beta$ = 91.96 (2)°, $V$ = 2672 (3) Å$^3$, and $Z$ = 4. In the solid state, the durene ring of **9** is nonplanar: the two unsubstituted durene ring carbon atoms are displaced out of the plane of the four methyl-substituted ring carbon atoms *toward* the rhodium center. Treatment of **2** with $HBF_4{\cdot}OEt_2$ yields an equilibrium mixture of ($\eta^5$-2,4-dimethylpentadienyl)Rh($PMe_3$)$_2$(H)$^+BF_4{}^-$ (**10**) and ($\eta^4$-2,4-dimethylpentadiene)Rh($PMe_3$)$_2{}^+BF_4{}^-$ (**11**). This mixture reacts with benzene and durene to produce ($\eta^6$-benzene)Rh($PMe_3$)$_2{}^+BF_4{}^-$ (**12**) and ($\eta^6$-durene)Rh($PMe_3$)$_2{}^+BF_4{}^-$ (**13**), respectively.

## Introduction

During the past several years, there has been increasing interest in the synthesis, structure, spectroscopy, and reactivity of metal complexes containing the acyclic pentadienyl ligand.[2] Our principal interest is in the *reactivity* of (pentadienyl)M complexes, and, for this reason, we have focussed our efforts on a new class of electron-rich (pentadienyl)M complexes—the pentadienyl–metal–tertiary phosphine complexes.[1] The tertiary phosphine ligands in these molecules serve three important functions. First, they promote electrophilic and oxidative addition reactions by increasing the electron density at the metal center. In so doing, they make it possible to introduce ligands such as hydrides and alkyls and probe the interactions of these ligands with the pentadienyl group. Second, they promote $\eta^5 \rightarrow \eta^3$ and $\eta^3 \rightarrow \eta^1$ pentadienyl ligand isomerizations by stabilizing the resulting coordinatively unsaturated metal centers. This enhances the reactivity of the complexes toward nucleophilic addition and substitution reactions. Third, because the steric and electronic features of phosphine ligands can be readily varied, they make it possible to change the environment at the metal center and probe the effect of such variations on reactivity.

Earlier, we reported the synthesis and dynamics of a new family of ($\eta^3$-2,4-dimethylpentadienyl)Rh($PR_3$)$_2$ complexes.[1h] We now wish to report reaction chemistry for two members of this family, ($\eta^3$-2,4-dimethylpentadienyl)Rh($PEt_3$)$_2$ (**1**) and ($\eta^3$-2,4-dimethylpentadienyl)Rh($PMe_3$)$_2$ (**2**).

## Results and Discussion

**Methylation of 1. Synthesis, Structure, and Dynamics of ($\eta^5$-2,4-Dimethylpentadienyl)Rh($PEt_3$)$_2$(Me)$^+O_3SCF_3{}^-$ (3).** Treatment of **1** with $CH_3{}^+O_3SCF_3{}^-$ results in methylation of the rhodium center and isomerization of the 2,4-dimethylpentadienyl ligand from $\eta^3$ to $\eta^5$ coordination to produce yellow ($\eta^5$-2,4-dimethylpentadienyl)Rh($PEt_3$)$_2$(Me)$^+O_3SCF_3{}^-$ (**3**) (see Scheme I).[3]

(1) The previous papers in this series are as follows: (a) Bleeke, J. R.; Kotyk, J. J. *Organometallics* **1983**, *2*, 1263. (b) Bleeke, J. R.; Hays, M. K. *Ibid.* **1984**, *3*, 506. (c) Bleeke, J. R.; Peng, W.-J. *Ibid.* **1984**, *3*, 1422. (d) Bleeke, J. R.; Kotyk, J. J. *Ibid.* **1985**, *4*, 194. (e) Bleeke, J. R.; Peng, W.-J. *Ibid.* **1986**, *5*, 635. (f) Bleeke, J. R.; Stanley, G. G.; Kotyk, J. J. *Ibid.* **1986**, *5*, 1642. (g) Bleeke, J. R.; Moore, D. A. *Inorg. Chem.* **1986**, *25*, 3522. (h) Bleeke, J. R.; Donaldson, A. J. *Organometallics* **1986**, *5*, 2401. (i) Bleeke, J. R.; Hays, M. K. *Ibid.* **1987**, *6*, 486. (j) Bleeke, J. R.; Kotyk, J. J.; Moore, D. A.; Rauscher, D. J. *J. Am. Chem. Soc.* **1987**, *109*, 417. (k) Bleeke, J. R.; Hays, M. K. *Organometallics* **1987**, *6*, 1367. (l) Bleeke, J. R.; Peng, W.-J. *Ibid.* **1987**, *6*, 1576. (m) Bleeke, J. R.; Donaldson, A. J.; Peng, W.-J. *Ibid.* **1988**, *7*, 33. (n) Bleeke, J. R.; Rauscher, D. J.; Moore, D. A. *Ibid.* **1987**, *6*, 2614. (o) Bleeke, J. R.; Hays, M. K.; Wittenbrink, R. J. *Ibid.* **1988**, *7*, 0000.

(2) (a) Ernst, R. D. *Acc. Chem. Res.* **1985**, *18*, 56. (b) Yasuda, H.; Nakamura, A. *J. Organomet. Chem.* **1985**, *285*, 15. (c) Powell, P. *Adv. Organomet. Chem.* **1986**, *26*, 125. (d) Lush, S.-F.; Liu, R.-S. *Organometallics* **1986**, *5*, 1908.

(3) Treatment of ($\eta^5$-cyclopentadienyl)Rh($PR_3$)$_2$ with $CH_3I$ produces ($\eta^5$-cyclopentadienyl)Rh($PR_3$)$_2$Me$^+I^-$: Werner, H.; Feser, R.; Buchner, W. *Chem. Ber.* **1979**, *112*, 834.

0276-7333/88/2307-1588$01.50/0 

**Table I. Positional Parameters and Their Estimated Standard Deviations for Non-Hydrogen Atoms in ($\eta^5$-2,4-Dimethylpentadienyl)Rh($PEt_3$)$_2$($CH_3$)$^+O_3SCF_3^-$ (3)**

| atom | x | y | z |
|---|---|---|---|
| Rh | 0.21161 (3) | 0.10311 (3) | 0.19033 (2) |
| P(1) | 0.2135 (1) | 0.2122 (1) | 0.09274 (9) |
| P(2) | 0.4030 (1) | 0.0339 (1) | 0.19642 (8) |
| C(1) | 0.0848 (6) | −0.0072 (5) | 0.1162 (4) |
| C(2) | 0.1187 (5) | −0.0525 (5) | 0.1838 (4) |
| C(3) | 0.1145 (5) | −0.0081 (5) | 0.2547 (3) |
| C(4) | 0.0730 (5) | 0.0865 (5) | 0.2696 (3) |
| C(5) | 0.0324 (5) | 0.1554 (6) | 0.2136 (4) |
| C(6) | 0.1695 (7) | −0.1554 (5) | 0.1848 (4) |
| C(7) | 0.0863 (7) | 0.1208 (6) | 0.3490 (4) |
| C(8) | 0.2902 (6) | 0.2125 (5) | 0.2608 (3) |
| C(11) | 0.1415 (6) | 0.1686 (6) | 0.0029 (4) |
| C(11)′ | 0.2081 (7) | 0.0910 (6) | −0.0358 (4) |
| C(12) | 0.3591 (5) | 0.2568 (5) | 0.0704 (3) |
| C(12)′ | 0.3598 (6) | 0.3282 (5) | 0.0057 (4) |
| C(13) | 0.1244 (6) | 0.3267 (6) | 0.0980 (5) |
| C(13)′ | 0.170 (1) | 0.4030 (6) | 0.1505 (7) |
| C(21) | 0.5302 (5) | 0.1188 (5) | 0.2075 (4) |
| C(21)′ | 0.6552 (6) | 0.0741 (7) | 0.2155 (6) |
| C(22) | 0.4371 (6) | −0.0502 (5) | 0.2751 (3) |
| C(22)′ | 0.4374 (7) | −0.0025 (7) | 0.3503 (4) |
| C(23) | 0.4262 (7) | −0.0395 (6) | 0.1144 (4) |
| C(23)′ | 0.4975 (9) | −0.1306 (7) | 0.1231 (6) |
| O(1) | 0.3607 (5) | 0.7738 (6) | 0.9472 (4) |
| O(2) | 0.1923 (7) | 0.7053 (5) | 0.8763 (3) |
| O(3) | 0.1635 (6) | 0.8213 (4) | 0.9644 (4) |
| S | 0.2420 (1) | 0.7497 (1) | 0.94217 (9) |
| C(9) | 0.2348 (6) | 0.6509 (6) | 1.0081 (4) |
| F(1) | 0.2770 (7) | 0.6745 (5) | 1.0738 (3) |
| F(2) | 0.1311 (6) | 0.6230 (5) | 1.0159 (4) |
| F(3) | 0.2987 (7) | 0.5767 (4) | 0.9962 (4) |

The $\eta^3 \rightarrow \eta^5$ isomerization of the 2,4-dimethylpentadienyl ligand enables the Rh(III) center in cation **3** to attain a stable 18e count.

An ORTEP drawing of the cation of **3**, derived from a single-crystal X-ray diffraction study, is shown in Figure 1. Positional parameters of the non-hydrogen atoms are listed in Table I, while important bond distances and angles are given in Table II. The overall coordination geometry of the cation of **3** is pseudooctahedral, with C(1), C(3), and C(5) of the 2,4-dimethylpentadienyl ligand, and P(1), P(2), and C(8) (methyl carbon) occupying the six coordination sites. The two phosphines reside in different chemical environments; P(1) sits under the open "mouth" of the 2,4-dimethylpentadienyl ligand, while P(2) resides under a 2,4-dimethylpentadienyl "edge". The methyl group occupies the other "edge" site. This geometry is

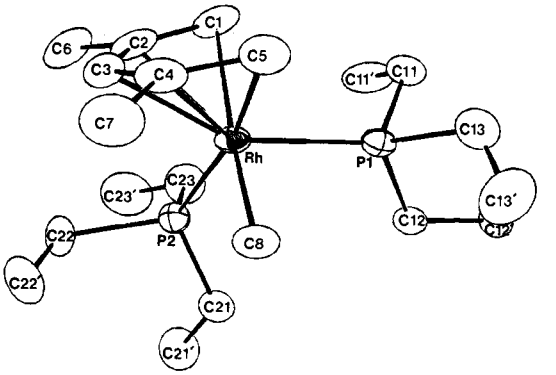


**Figure 1.** ORTEP drawing of cation of ($\eta^5$-2,4-dimethylpentadienyl)Rh($PEt_3$)$_2$($CH_3$)$^+O_3SCF_3^-$ (**3**).

**Scheme I**[a]

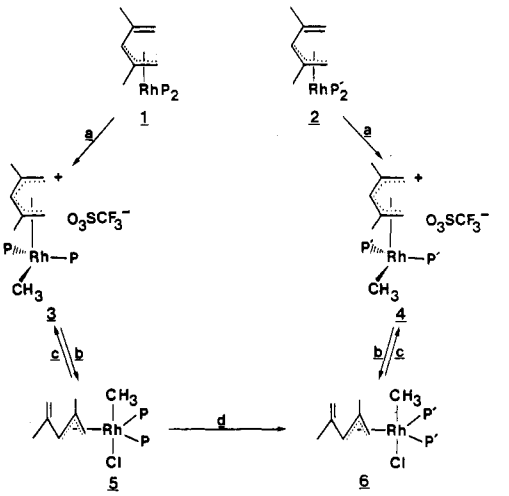


[a] P = $Et_3$; P′ = $PMe_3$. (a) $CH_3^+O_3SCF_3^-$. (b) $(Ph_3P)_2N^+Cl^-$. (c) $Ag^+O_3SCF_3^-$. (d) 2 equiv of $PMe_3$.

probably dictated by steric considerations; i.e., the largest ligand ($PEt_3$) resides in the roomiest coordination site (under the "mouth"). Interestingly, the Rh–$C_{pentadienyl}$ distances decrease monotonically in going from C(1) to C(5). Hence, Rh–C(1) is the longest bond (2.387 (6) Å) and Rh–C(5) is the shortest (2.228 (6) Å). This effect may arise from stronger back-bonding into the $\pi^*$ orbitals on the 2,4-dimethylpentadienyl carbon atoms trans to $PEt_3$ (C(5) and C(4)).[4] Consistent with this explanation is the fact

**Table II. Selected Bond Distances (Å) and Bond Angles (deg) with Estimated Standard Deviations for ($\eta^5$-2,4-Dimethylpentadienyl)Rh($PEt_3$)$_2$($CH_3$)$^+O_3SCF_3^-$ (3)**

| | | | | | |
|---|---|---|---|---|---|
| **Bond Distances** | | | | | |
| Rh–P(1) | 2.311 (2) | Rh–C(8) | 2.094 (6) | C(4)–C(7) | 1.513 (8) |
| Rh–P(2) | 2.350 (1) | C(1)–C(2) | 1.394 (10) | P–C[a] | 1.84 (2) |
| Rh–C(1) | 2.387 (6) | C(2)–C(3) | 1.428 (8) | phosphine C–C[a] | 1.50 (2) |
| Rh–C(2) | 2.347 (6) | C(2)–C(6) | 1.504 (10) | S–O[b] | 1.39 (1) |
| Rh–C(3) | 2.260 (6) | C(3)–C(4) | 1.397 (9) | S–C | 1.803 (8) |
| Rh–C(4) | 2.251 (5) | C(4)–C(5) | 1.422 (9) | C–F[b] | 1.27 (1) |
| Rh–C(5) | 2.228 (6) | | | | |
| **Bond Angles** | | | | | |
| P(1)–Rh–P(2) | 101.99 (5) | P(2)–Rh–C(8) | 85.5 (2) | C(1)–C(2)–C(3) | 125.7 (7) |
| P(1)–Rh–C(1) | 90.9 (2) | C(1)–Rh–C(3) | 65.3 (2) | C(1)–C(2)–C(6) | 119.1 (6) |
| P(1)–Rh–C(3) | 150.1 (2) | C(1)–Rh–C(5) | 78.5 (3) | C(3)–C(2)–C(6) | 115.2 (6) |
| P(1)–Rh–C(5) | 91.5 (2) | C(1)–Rh–C(8) | 168.3 (2) | C(2)–C(3)–C(4) | 127.1 (6) |
| P(1)–Rh–C(8) | 89.2 (2) | C(3)–Rh–C(5) | 67.1 (2) | C(3)–C(4)–C(5) | 123.3 (5) |
| P(2)–Rh–C(1) | 106.0 (2) | C(3)–Rh–C(8) | 110.4 (2) | C(3)–C(4)–C(7) | 117.7 (6) |
| P(2)–Rh–C(3) | 101.9 (2) | C(5)–Rh–C(8) | 89.8 (2) | C(5)–C(4)–C(7) | 118.6 (6) |
| P(2)–Rh–C(5) | 165.6 (2) | | | | |

[a] Average of six values. [b] Average of three values.

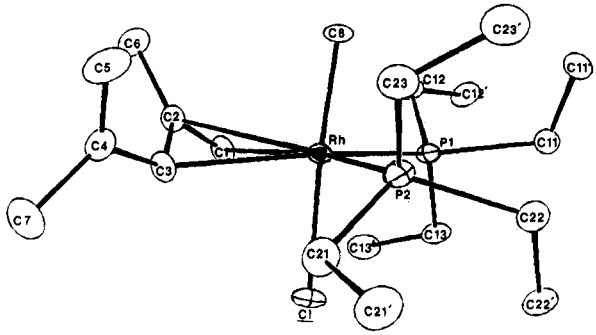


**Figure 2.** ORTEP drawing of ($\eta^3$-2,4-dimethylpentadienyl)Rh($PEt_3$)$_2$($CH_3$)(Cl) (**5**). The ethyl group, C(23)–C(23)′, exhibits a twofold disorder in the solid state, and only one set of carbon atoms, C(23)A–C(23)C, has been included in the drawing.

**Scheme II**

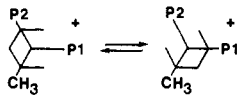


that C(4)–C(5) is somewhat longer than C(1)–C(2) (1.422 (9) Å vs 1.394 (10) Å).

The unsymmetrical structure of cation **3** is retained in solution at 20 °C. Hence at 20 °C, the $^{31}P\{^1H\}$ NMR spectrum consists of two signals (both are doublets of doublets due to $^{103}Rh$ and $^{31}P$ coupling), while the $^{13}C\{^1H\}$ spectrum exhibits seven independent signals for the 2,4-dimethylpentadienyl ligand. However, as the sample is heated in solution, the 2,4-dimethylpentadienyl ligand begins to rotate with respect to the $RhP_2(Me)$ framework (see Scheme II). This rotational process,[1f] which exchanges the two phosphine ligands, as well as the ends of the 2,4-dimethylpentadienyl ligand, has a free energy of activation, $\Delta G^{\ddagger}$, of 17.0 ± 0.7 kcal/mol at 75 °C.

**Methylation of 2. Synthesis of ($\eta^5$-2,4-Dimethylpentadienyl)Rh($PMe_3$)$_2$(Me)$^+O_3SCF_3^-$ (4).** ($\eta^3$-2,4-Dimethylpentadienyl)Rh($PMe_3$)$_2$ (**2**) also reacts cleanly with $CH_3{}^+O_3SCF_3^-$ to produce the $PMe_3$ analogue of **3**, ($\eta^5$-2,4-dimethylpentadienyl)Rh($PMe_3$)$_2$(Me)$^+O_3SCF_3^-$ (**4**). As in **3**, the phosphine ligands and the ends of the pentadienyl group in **4** are inequivalent by NMR at 20 °C, indicating an unsymmetrical ground-state structure with a phosphine ligand residing under the 2,4-dimethylpentadienyl "mouth". However, pentadienyl ligand rotation in **4** (cf. Scheme II) is not observed even upon heating to 80 °C. The higher barrier to pentadienyl ligand rotation exhibited by **4** (vs **3**) suggests that rotation *may* proceed through a 16e ($\eta^3$-2,4-dimethylpentadienyl)Rh($PR_3$)$_2$(Me)$^+$ intermediate.[1f,g] Such an intermediate would be expected to be more accessible in the more sterically congested $PEt_3$ system.

**Reaction of 3 with $(Ph_3P)_2N^+Cl^-$. Synthesis, Structure, and Dynamics of ($\eta^3$-2,4-Dimethylpentadienyl)Rh($PEt_3$)$_2$(Me)(Cl) (5).** Treatment of ($\eta^5$-2,4-dimethylpentadienyl)Rh($PEt_3$)$_2$(Me)$^+O_3SCF_3^-$ (**3**) with $(Ph_3P)_2N^+Cl^-$ (PPN$^+$Cl$^-$) produces yellow ($\eta^3$-2,4-dimethylpentadienyl)Rh($PEt_3$)$_2$(Me)(Cl) (**5**).[5] An ORTEP drawing of **5**, derived from an X-ray diffraction study, is shown in Figure 2. Positional parameters of non-hydrogen atoms are listed in Table III, while significant bond distances and angles are given in Table IV. The coordination geometry is octahedral, with C(1) and C(3) (2,4-dimethylpentadienyl group), P(1), P(2), C(8) (methyl carbon), and Cl occupying the six coordination sites. The phosphines are trans to the 2,4-dimethylpentadienyl group, while the methyl and chloro ligands reside trans to one another. The "mouth" of the $\eta^3$-2,4-dimethylpentadienyl ligand opens toward the chloro ligand and away from the methyl group.

The 2,4-dimethylpentadienyl ligand has a syn geometry; i.e., the isopropenyl group is syn to the hydrogen on C(2) and is sickle-shaped (torsional angle C(2)–C(3)–C(4)–C(5) equals 49.1°). All previous examples of *syn*-$\eta^3$-pentadienyl[1b,d,6] and *syn*-$\eta^3$-2,4-dimethylpentadienyl[1e] ligands have crystallized in a W shape with a C(2)–C(3)–C(4)–C(5) torsional angle between 145° and 170°. C(1), C(2), C(3), and C(4) are planar to within 0.013 Å. C(5) lies 0.80 Å out of this plane in the direction of the Rh atom, while C(7) lies 1.00 Å out of the plane in the opposite direction.

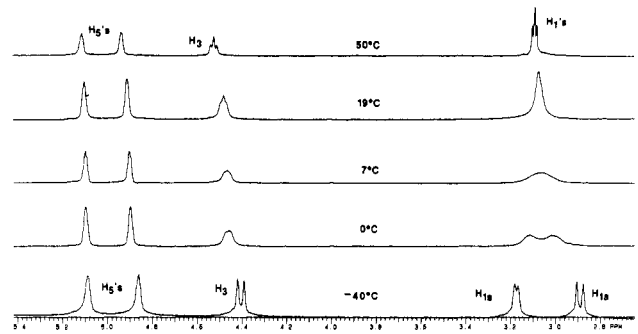


**Figure 3.** Pentadienyl region of 300-MHz $^1H$ NMR spectrum of ($\eta^3$-2,4-dimethylpentadienyl)Rh($PEt_3$)$_2$(Me)(Cl) (**5**) at −40 °C (very slow exchange), 0 °C, 7 °C (coalescence), 19 °C, and 50 °C (fast exchange). The dynamic process that exchanges $H(1)_s$ and $H(1)_a$ involves a C(1)-bound ($\eta^1$-dimethylpentadienyl)Rh intermediate.

**Scheme III**

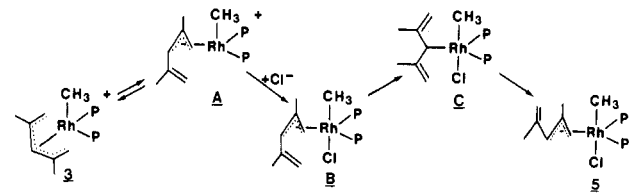


**Scheme IV**

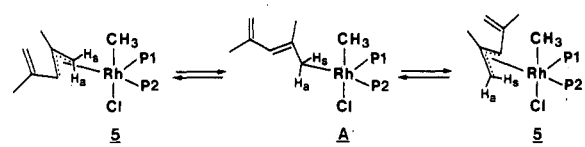


(4) On the basis of trans influence, a trend in the other direction is anticipated. The methyl ligand exerts a weaker trans influence than the $PEt_3$ ligand; hence, the ligand trans to methyl (C(1)) should reside closer to Rh than the ligand trans to $PEt_3$ (C(5)). See: Appleton, T. G.; Clark, H. C.; Manzer, L. E. *Coord. Chem. Rev.* **1973**, *10*, 335.

(5) (a) In a related reaction, Powell has shown that [($\eta^5$-1-arylpentadienyl)($\eta^5$-cyclopentadienyl)Rh]$^+$ reacts with Cl$^-$ to produce (*anti*-$\eta^3$-arylpentadienyl)($\eta^5$-cyclopentadienyl)Rh(Cl): Powell, P.; Stephens, M.; Muller, A. *J. Organomet. Chem.* **1986**, *318*, 255. (b) This reaction also bears some resemblance to the reaction of [($\eta^2$-*o*-$BrC_6H_4PPh_2$)Ir($\eta^4$-cyclooctadiene)]$^+$ with Cl$^-$ to produce ($\eta^1$-*o*-$BrC_6H_4PPh_2$)Ir(Cl)($\eta^4$-cyclooctadiene). In this system, chloride addition is preceded by dissociation of the pendant bromo group: Burk, M. J.; Crabtree, R. H.; Holt, E. M. *Organometallics* **1984**, *3*, 638.

(6) (a) Lee, G.-H.; Peng, S.-M.; Liao, M.-Y.; Liu, R.-S. *J. Organomet. Chem.* **1986**, *312*, 113. (b) Lee, G.-H.; Peng, S.-M.; Lee, T.-W.; Liu, R.-S. *Organometallics* **1986**, *5*, 2378.

**Table III. Positional Parameters and Their Estimated Standard Deviations for Non-Hydrogen Atoms in ($\eta^3$-2,4-Dimethylpentadienyl)Rh($PEt_3$)$_2$($CH_3$)(Cl) (5)**

| atom | x | y | z |
|---|---|---|---|
| Rh | 0.30643 (2) | 0.11901 (4) | 0.15497 (1) |
| Cl | 0.2421 (1) | 0.3854 (1) | 0.19371 (5) |
| P(1) | 0.18752 (8) | −0.0220 (1) | 0.20579 (5) |
| P(2) | 0.22114 (9) | 0.1918 (2) | 0.06388 (5) |
| C(1) | 0.4199 (4) | 0.1170 (5) | 0.2300 (2) |
| C(2) | 0.4798 (3) | 0.1384 (5) | 0.1806 (2) |
| C(3) | 0.4552 (3) | 0.2723 (6) | 0.1437 (2) |
| C(4) | 0.5107 (3) | 0.3182 (6) | 0.0913 (2) |
| C(5) | 0.5335 (4) | 0.2160 (8) | 0.0482 (3) |
| C(6) | 0.5621 (4) | 0.0174 (7) | 0.1694 (3) |
| C(7) | 0.5363 (5) | 0.4947 (7) | 0.0889 (3) |
| C(8) | 0.3495 (4) | −0.1055 (5) | 0.1216 (2) |
| C(11) | 0.0678 (4) | −0.1051 (6) | 0.1681 (2) |
| C(11)′ | 0.0800 (4) | −0.2356 (7) | 0.1228 (3) |
| C(12) | 0.2402 (3) | −0.2009 (6) | 0.2452 (2) |
| C(12)′ | 0.1689 (4) | −0.2895 (7) | 0.2842 (3) |
| C(13) | 0.1284 (4) | 0.0936 (6) | 0.2632 (2) |
| C(13)′ | 0.1994 (5) | 0.1442 (7) | 0.3155 (2) |
| C(21) | 0.2544 (4) | 0.4010 (7) | 0.0440 (2) |
| C(21)′ | 0.1919 (5) | 0.4852 (8) | −0.0059 (3) |
| C(22) | 0.0796 (4) | 0.1880 (7) | 0.0535 (2) |
| C(22)′ | 0.0243 (4) | 0.2969 (7) | 0.0950 (2) |
| C(23)A[a] | 0.2672 (8) | 0.115 (1) | −0.0063 (5) |
| C(23)B[a] | 0.2548 (7) | 0.039 (1) | 0.0057 (4) |
| C(23)C[b] | 0.201 (1) | −0.031 (2) | −0.0333 (7) |
| C(23)D[b] | 0.205 (1) | 0.062 (2) | −0.0566 (6) |

[a] Carbon atom C(23) exhibited a twofold disorder. C(23)A and C(23)B were refined with multiplicities of 0.5. [b] Carbon atom C(23)′ exhibited a twofold disorder. C(23)C and C(23)D were refined with multiplicities of 0.5.

As outlined in Scheme III, we propose that the reaction of **3** with $PPN^+Cl^-$ proceeds through the intermediacy of 16e (*anti*-$\eta^3$-2,4-dimethylpentadienyl)Rh($PEt_3$)$_2$$Me^+$ (A, Scheme III), which is attacked by $Cl^-$. The resulting (*anti*-$\eta^3$-2,4-dimethylpentadienyl)Rh($PEt_3$)$_2$(Me)(Cl) complex (B, Scheme III) can then rapidly rearrange to (*syn*-$\eta^3$-2,4-dimethylpentadienyl)Rh($PEt_3$)$_2$(Me)(Cl) (**5**) via a C(3)-bound $\eta^1$-2,4-dimethylpentadienyl intermediate C, Scheme III).[7]

In solution, as in the solid state, **5** adopts the syn-$\eta^3$ configuration. None of the anti-$\eta^3$ isomer is detectable by NMR. Furthermore, the isomerization of **5** to C (see Scheme III), which would exchange the ends of the 2,4-dimethylpentadienyl ligand (C(1) and C(5)), is not observed by NMR. However, a related dynamic process, the isomerization of **5** to the C(1)-bound $\eta^1$-2,4-dimethylpentadienyl complex (A, Scheme IV),[8] can be detected by NMR in the temperature range −80 → 50 °C. This process exchanges the two hydrogens on C(1) of the 2,4-dimethylpentadienyl ligand as well as the two $PEt_3$ ligands.[9] The variable-temperature $^1H$ NMR signals for the 2,4-dimethylpentadienyl ligand in **5** are shown in Figure 3. At −40 °C, the complex is in very slow exchange and the two hydrogens on C(1) ($H(1)_{syn}$ and $H(1)_{anti}$) appear as distinct signals. Each is a doublet as a result of coupling to the trans phosphorus, P(2). Furthermore, H(3) is a doublet as a result of coupling to its trans phosphorus, P(1). As the temperature is raised, the signals due to $H(1)_{syn}$ and $H(1)_{anti}$ broaden and coalesce (at 7 °C). Further warming to 50 °C causes this coalesced signal to sharpen to a triplet, due to coupling to the two equivalent phosphorus nuclei. Similarly, the signal for H(3) becomes a triplet at 50 °C.[10] Using the coalescence temperature and the peak separation of $H(1)_{syn}$ and $H(1)_{anti}$ at the stopped exchange limit (−80 °C), we have calculated a free energy of activation, $\Delta G^{\ddagger}$, of 13.0 ± 0.5 kcal/mol for this $\eta^3 \rightleftharpoons \eta^1 \rightleftharpoons \eta^3$ fluxional process. As shown in Scheme I, **5** is converted back to **3** upon treatment with $Ag^+O_3SCF_3^-$.

**Scheme V**[a]

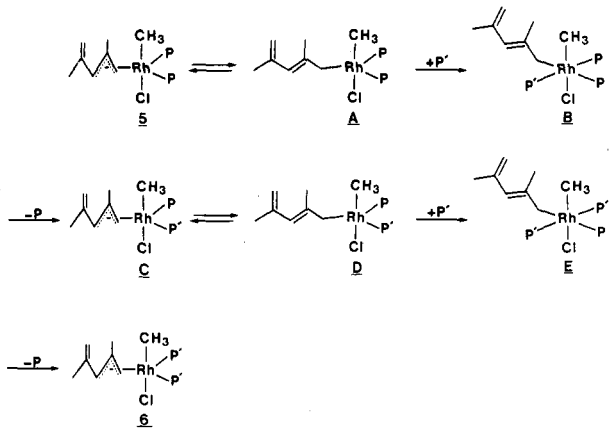


[a] P = $PEt_3$; P′ = $PMe_3$.

**Reaction of 4 with $(Ph_3P)_2N^+Cl^-$. Synthesis of ($\eta^3$-2,4-Dimethylpentadienyl)Rh($PMe_3$)$_2$(Me)(Cl) (6).** Treatment of ($\eta^5$-2,4-dimethylpentadienyl)Rh($PMe_3$)$_2$(Me)$^+O_3SCF_3^-$ (**4**) with $(Ph_3P)_2N^+Cl^-$ produces the $PMe_3$ analogue of **5**, ($\eta^3$-2,4-dimethylpentadienyl)Rh($PMe_3$)$_2$(Me)(Cl) (**6**). NMR spectra of **6** closely resemble the stopped-exchange spectra of **5**, strongly suggesting that **6** and **5** possess the same ground-state structure. However, unlike **5**, **6** does not exhibit the $\eta^3 \rightleftharpoons \eta^1 \rightleftharpoons \eta^3$ dynamic process (cf. Scheme IV) in solution at 20 °C; i.e., $H(1)_{syn}$ and $H(1)_{anti}$ signals show no broadening due to site exchange. This higher activation energy for the $\eta^3 \rightleftharpoons \eta^1$ 2,4-dimethylpentadienyl isomerization in **6** (as compared to **5**) is again attributable to decreased steric interactions involving the smaller $PMe_3$ ligands.[11] As shown in Scheme I, **6** can be reconverted to **4** by treatment with $Ag^+O_3SCF_3^-$.

**Reaction of 5 with $PMe_3$.** ($\eta^3$-2,4-Dimethylpentadienyl)Rh($PEt_3$)$_2$(Me)(Cl) (**5**) is susceptible to nucleophilic attack in solution because 16e ($\eta^1$-2,4-dimethylpentadienyl)Rh intermediates are accessible (Scheme IV). For example, **5** reacts with 2 equiv of $PMe_3$ to produce the phosphine-exchanged complex, ($\eta^3$-2,4-dimethylpentadienyl)Rh($PMe_3$)$_2$(Me)(Cl) (**6**). The putative mechanism for this reaction, shown in Scheme V, involves a series of associative steps, which are preceded by $\eta^3 \rightarrow \eta^1$ 2,4-dimethylpentadienyl ligand isomerizations. The mixed-phosphine complex, ($\eta^3$-2,4-dimethylpentadienyl)Rh($PEt_3$)($PMe_3$)(Me)(Cl) (C, Scheme V), has been detected by NMR. Not surprisingly, **6** *cannot* be reconverted to **5** by reaction with excess $PEt_3$. (Recall that **6** does not

(7) We have postulated a similar C(3)-bound ($\eta^1$-2,4-dimethylpentadienyl)M intermediate in the isomerization of (*anti*-$\eta^3$-2,4-dimethylpentadienyl)Co($PMe_3$)$_3$ to its syn-$\eta^3$ isomer. See ref 1c.

(8) Several stable C(1)-bound ($\eta^1$-pentadienyl)M complexes have been isolated. See ref 1n, 2d, and 6a,b. See also: (a) Yasuda, H.; Nagasuna, K.; Akita, M.; Lee, K.; Nakamura, A. *Organometallics* **1984**, *3*, 1470. (b) Lee, T.-W.; Liu, R.-S. *J. Organomet. Chem.* **1987**, *320*, 211.

(9) Similar $\eta^3 \rightleftharpoons \eta^1 \rightleftharpoons \eta^3$ dynamic processes are quite common in (allyl)M chemistry. (a) Tsutsui, M.; Courtney, A. In *Advances in Organometallic Chemistry*; Stone, F. G. A., West, R., Eds.; Academic: New York, 1977; Vol. 16, p 241. (b) Vrieze, K. In *Dynamic Nuclear Magnetic Resonance*; Jackman, L. M., Cotton, F. A., Eds.; Academic: New York, 1975; p 441. (c) Egan, J. W., Jr.; Hughes, R. P.; Rheingold, A. L. *Organometallics* **1987**, *6*, 1578.

(10) In the $^{13}C\{^1H\}$ NMR spectrum, the signals for C(1) and C(3) also change from doublets at −20 °C (very slow exchange) to triplets at 20 °C (fast exchange).

(11) $PEt_3$ has a cone angle of 132° compared to a cone angle of 118° for $PMe_3$: Tolman, C. A. *Chem. Rev.* **1977**, *77*, 313.

**Table IV. Selected Bond Distances (Å) and Bond Angles (deg) with Estimated Standard Deviations for ($\eta^3$-2,4-Dimethylpentadienyl)Rh($PEt_3$)$_2$($CH_3$)(Cl) (5)**

| | | | | | |
|---|---|---|---|---|---|
| **Bond Distances** | | | | | |
| Rh–Cl | 2.528 (1) | Rh–C(3) | 2.335 (4) | C(3)–C(4) | 1.486 (7) |
| Rh–P(1) | 2.307 (1) | Rh–C(8) | 2.090 (4) | C(4)–C(5) | 1.342 (9) |
| Rh–P(2) | 2.355 (1) | C(1)–C(2) | 1.424 (7) | C(4)–C(7) | 1.492 (10) |
| Rh–C(1) | 2.171 (5) | C(2)–C(3) | 1.408 (6) | P–C[a,b] | 1.85 (2) |
| Rh–C(2) | 2.285 (4) | C(2)–C(6) | 1.495 (8) | phosphine C–C[a,b] | 1.52 (3) |
| **Bond Angles** | | | | | |
| Cl–Rh–P(1) | 90.70 (4) | P(1)–Rh–C(8) | 86.7 (2) | C(1)–C(2)–C(3) | 117.1 (5) |
| Cl–Rh–P(2) | 86.58 (4) | P(2)–Rh–C(1) | 160.4 (1) | C(1)–C(2)–C(6) | 119.2 (5) |
| Cl–Rh–C(1) | 87.4 (2) | P(2)–Rh–C(3) | 96.0 (1) | C(3)–C(2)–C(6) | 123.6 (5) |
| Cl–Rh–C(3) | 82.3 (1) | P(2)–Rh–C(8) | 91.5 (2) | C(2)–C(3)–C(4) | 125.2 (5) |
| Cl–Rh–C(8) | 176.2 (2) | C(1)–Rh–C(3) | 64.7 (2) | C(3)–C(4)–C(5) | 124.9 (5) |
| P(1)–Rh–P(2) | 106.35 (4) | C(1)–Rh–C(8) | 95.5 (2) | C(3)–C(4)–C(7) | 113.5 (6) |
| P(1)–Rh–C(1) | 92.3 (1) | C(3)–Rh–C(8) | 101.2 (2) | C(5)–C(4)–C(7) | 121.5 (6) |
| P(1)–Rh–C(3) | 156.2 (1) | | | | |

[a] Includes both sets of distances for the disordered ethyl group, C(23)–C(23)′. [b] Average of seven values.

**Scheme VI**[a]

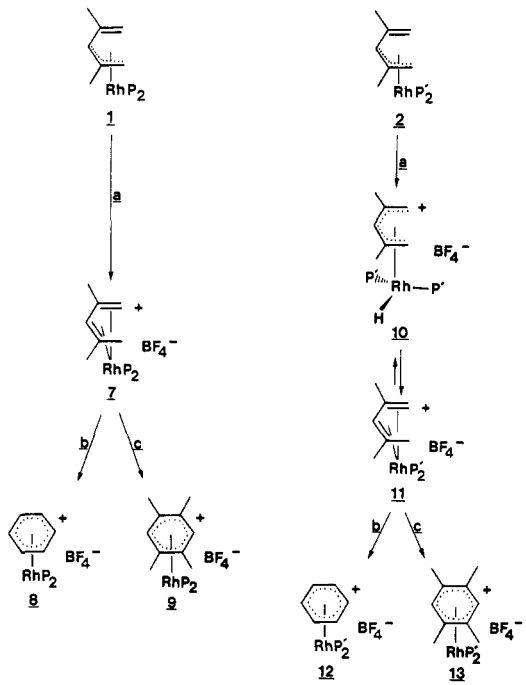


[a] P = $PEt_3$; P′ = $PMe_3$. (a) $HBF_4{\cdot}OEt_2$. (b) Benzene. (c) Durene.

readily undergo the $\eta^3 \rightleftharpoons \eta^1$ pentadienyl ligand shift in solution.)

**Protonation of 1.** Treatment of ($\eta^3$-2,4-dimethylpentadienyl)Rh($PEt_3$)$_2$ (1) with $HBF_4{\cdot}OEt_2$ produces red ($\eta^4$-2,4-dimethylpentadiene)Rh($PEt_3$)$_2^+BF_4^-$ (7) (see Scheme VI). This reaction probably proceeds by initial protonation at the rhodium center (vide infra),[12,13] followed by rapid migration of the resulting hydride to C(1) of the 2,4-dimethylpentadienyl ligand. Concomitantly, the rhodium center coordinates the dangling double bond of the diene.

Although 7 is stable for a short time in tetrahydrofuran solution, its extreme susceptibility to loss of 2,4-dimethylpentadiene has frustrated attempts to isolate it as a solid. However, 7 reacts quantitatively in situ with arenes, releasing 2,4-dimethylpentadiene and producing 18e ($\eta^6$-arene)Rh($PEt_3$)$_2^+BF_4^-$ complexes. Using this approach, we have synthesized ($\eta^6$-benzene)Rh($PEt_3$)$_2^+BF_4^-$ (8) and ($\eta^6$-durene)Rh($PEt_3$)$_2^+BF_4^-$ (9).[14]

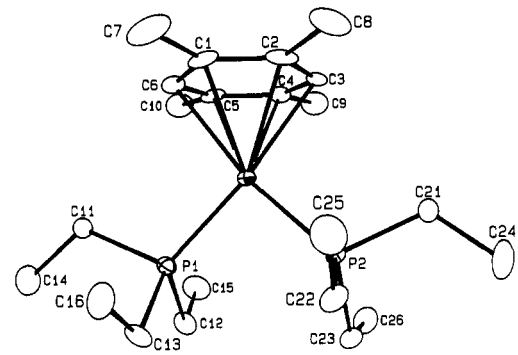


**Figure 4.** ORTEP drawing of cation in ($\eta^6$-durene)Rh($PEt_3$)$_2^+BF_4^-$ (9).

**Table V. Positional Parameters and Their Estimated Standard Deviations for Non-Hydrogen Atoms in ($\eta^6$-Durene)Rh($PEt_3$)$_2^+BF_4^-$ (9)**

| atom | *x* | *y* | *z* |
|---|---|---|---|
| Rh | 0.12026 (7) | 0.20076 (7) | 0.37439 (3) |
| P(1) | 0.3035 (3) | 0.0568 (3) | 0.3577 (1) |
| P(2) | 0.3045 (3) | 0.3337 (3) | 0.4024 (1) |
| C(1) | −0.117 (1) | 0.130 (1) | 0.4082 (4) |
| C(2) | −0.112 (1) | 0.259 (1) | 0.4125 (4) |
| C(3) | −0.097 (1) | 0.332 (1) | 0.3714 (5) |
| C(4) | −0.098 (1) | 0.281 (1) | 0.3282 (4) |
| C(5) | −0.104 (1) | 0.155 (1) | 0.3246 (4) |
| C(6) | −0.101 (1) | 0.081 (1) | 0.3649 (4) |
| C(7) | −0.141 (2) | 0.046 (2) | 0.4491 (6) |
| C(8) | −0.138 (2) | 0.321 (2) | 0.4572 (6) |
| C(9) | −0.105 (2) | 0.362 (1) | 0.2872 (5) |
| C(10) | −0.117 (2) | 0.093 (2) | 0.2801 (5) |
| C(11) | 0.206 (1) | −0.088 (1) | 0.3411 (5) |
| C(12) | 0.434 (1) | 0.086 (1) | 0.3106 (4) |
| C(13) | 0.451 (1) | 0.009 (1) | 0.4012 (5) |
| C(14) | 0.317 (2) | −0.193 (1) | 0.3276 (6) |
| C(15) | 0.348 (2) | 0.113 (2) | 0.2685 (5) |
| C(16) | 0.378 (2) | −0.040 (1) | 0.4426 (6) |
| C(21) | 0.222 (1) | 0.486 (1) | 0.4110 (5) |
| C(22) | 0.395 (1) | 0.301 (1) | 0.4594 (4) |
| C(23) | 0.483 (1) | 0.368 (1) | 0.3691 (4) |
| C(24) | 0.334 (2) | 0.584 (1) | 0.4312 (6) |
| C(25) | 0.285 (2) | 0.283 (2) | 0.4949 (5) |
| C(26) | 0.449 (2) | 0.419 (1) | 0.3234 (6) |
| B | 0.696 (2) | 0.206 (2) | 0.1403 (7) |
| F(1) | 0.766 (3) | 0.301 (2) | 0.1369 (8) |
| F(2) | 0.782 (2) | 0.115 (2) | 0.1214 (7) |
| F(3) | 0.563 (3) | 0.163 (3) | 0.157 (1) |
| F(4) | 0.598 (3) | 0.237 (2) | 0.1032 (8) |

(12) Most protonations of electron-rich polyenyl–metal complexes involve initial attack at the metal center. See, for example, (a) Byrne, J. W.; Blaser, H. U.; Osborn, J. A. *J. Am. Chem. Soc.* **1975**, *97*, 3871. (b) Nixon, J. F.; Wilkins, B. *J. Organomet. Chem.* **1974**, *80*, 129. (c) Ittel, S. D.; VanCatledge, F. A.; Jesson, J. P. *J. Am. Chem. Soc.* **1979**, *101*, 6905.

(13) Werner has demonstrated that protonation of ($\eta^5$-cyclopentadienyl)Rh($PR_3$)$_2$ produces ($\eta^5$-cyclopentadienyl)Rh($PR_3$)$_2$(H)$^+$. See ref 3.

Table VI. Selected Bond Distances (Å) and Bond Angles (deg) with Estimated Standard Deviations for ($\eta^6$-Durene)Rh($PEt_3$)$_2^+BF_4^-$ (9)

| | | | | | |
|---|---|---|---|---|---|
| **Bond Distances** | | | | | |
| Rh-P(1) | 2.251 (2) | Rh-C(6) | 2.266 (6) | C(4)-C(5) | 1.368 (11) |
| Rh-P(2) | 2.246 (2) | C(1)-C(2) | 1.404 (12) | C(4)-C(9) | 1.498 (11) |
| Rh-C(1) | 2.373 (6) | C(1)-C(6) | 1.396 (11) | C(5)-C(6) | 1.435 (10) |
| Rh-C(2) | 2.360 (6) | C(1)-C(7) | 1.536 (11) | C(5)-C(10) | 1.476 (11) |
| Rh-C(3) | 2.310 (6) | C(2)-C(3) | 1.459 (11) | P-C[a] | 1.83 (2) |
| Rh-C(4) | 2.403 (7) | C(2)-C(8) | 1.503 (12) | phosphine C-C[a] | 1.48 (2) |
| Rh-C(5) | 2.395 (6) | C(3)-C(4) | 1.393 (11) | B-F[b] | 1.31 (3) |
| **Bond Angles** | | | | | |
| P(1)-Rh-P(2) | 93.64 (6) | P(2)-Rh-C(3) | 98.4 (2) | C(6)-C(1)-C(2) | 117.9 (7) |
| P(1)-Rh-C(1) | 116.9 (2) | P(2)-Rh-C(4) | 118.3 (2) | C(2)-C(1)-C(7) | 121.8 (9) |
| P(1)-Rh-C(2) | 149.9 (2) | P(2)-Rh-C(5) | 150.6 (2) | C(1)-C(2)-C(8) | 121.3 (9) |
| P(1)-Rh-C(3) | 163.6 (2) | P(2)-Rh-C(6) | 163.3 (2) | C(3)-C(2)-C(8) | 120.6 (9) |
| P(1)-Rh-C(4) | 129.4 (2) | C(1)-C(2)-C(3) | 117.8 (7) | C(3)-C(4)-C(9) | 120.1 (7) |
| P(1)-Rh-C(5) | 104.3 (2) | C(2)-C(3)-C(4) | 123.2 (7) | C(9)-C(4)-C(5) | 121.8 (8) |
| P(1)-Rh-C(6) | 97.6 (2) | C(3)-C(4)-C(5) | 118.0 (7) | C(4)-C(5)-C(10) | 121.4 (8) |
| P(2)-Rh-C(1) | 128.5 (2) | C(4)-C(5)-C(6) | 119.7 (7) | C(10)-C(5)-C(6) | 118.9 (7) |
| P(2)-Rh-C(2) | 102.4 (2) | C(5)-C(6)-C(1) | 122.9 (7) | C(6)-C(1)-C(7) | 120.7 (8) |

[a] Average of six values. [b] Average of four values.

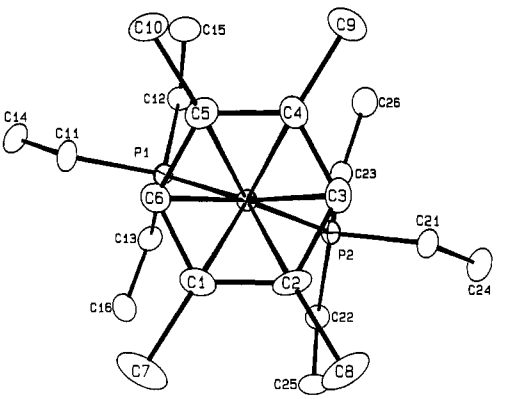


**Figure 5.** "Overhead" view of cation in ($\eta^6$-durene)Rh($PEt_3$)$_2^+$-$BF_4^-$ (9), showing projection of Rh-P vectors onto durene ring.

An ORTEP drawing of 9, derived from a single-crystal X-ray diffraction study, is shown in Figure 4. Positional parameters of non-hydrogen atoms are listed in Table V, while significant bond distances and angles are given in Table VI. The projection of the $PEt_3$ ligands onto the durene ring can be clearly seen in the "overhead" view of 9, shown in Figure 5. The dihedral angle between the planes defined by C(3)/C(6)/Rh and P(1)/P(2)/Rh is 19.7 (5)°. The unsubstituted ring carbon atoms, C(3) and C(6), are displaced out of the plane of the four methyl-substituted ring carbon atoms, C(1), C(2), C(4), and C(5), *toward* the rhodium center.[15] As a result, the average Rh-C distance for the unsubstituted ring carbons is 2.29 (1) Å, while that for the methyl-substituted ring carbons is 2.38 (1) Å. Furthermore, ring C-C bonds C(2)-C(3) and C(5)-C(6), which are "eclipsed" by Rh-P vectors (see Figure 5), are slightly longer than the "uneclipsed" bonds, C(1)-C(2), C(3)-C(4), C(4)-C(5), and C(6)-C(1) (average distances are 1.45 (1) Å for "eclipsed" and 1.39 (2) Å for "uneclipsed").

**Protonation of 2.** When ($\eta^3$-2,4-dimethylpentadienyl)Rh($PMe_3$)$_2$ (2) is treated with $HBF_4$·$OEt_2$, a 30:70 equilibrium mixture of ($\eta^5$-2,4-dimethylpentadienyl)Rh($PMe_3$)$_2$(H)$^+BF_4^-$ (10) and ($\eta^4$-2,4-dimethylpentadiene)Rh($PMe_3$)$_2^+BF_4^-$ (11) is produced (see Scheme VI). By NMR, 10 adopts the same unsymmetrical ground-state structure that we observed earlier for methylation products 3 and 4; i.e., the two $PMe_3$ ligands reside in different chemical environments—one under the open "mouth" of the 2,4-dimethylpentadienyl ligand and one under a 2,4-dimethylpentadienyl "edge". The hydride occupies the other "edge" site. As indicated in Scheme VI, 10 is probably an intermediate along the pathway to 11; i.e., protonation probably occurs initially at the rhodium center and is followed by hydride migration to C(1) of the 2,4-dimethylpentadienyl ligand.[12,13]

Treatment of the equilibrium mixture of 10 and 11 with an arene leads to quantitative displacement of 2,4-dimethylpentadiene and production of ($\eta^6$-arene)Rh($PMe_3$)$_2^+BF_4^-$. The arene probably reacts exclusively with 16e 11; this, in turn, drives the 10 ⇌ 11 equilibrium from left to right. Among the (arene)Rh complexes that we have synthesized by this route are ($\eta^6$-benzene)Rh($PMe_3$)$_2^+$ $BF_4^-$ (12) and ($\eta^6$-durene)Rh($PMe_3$)$_2^+BF_4^-$ (13).[14]

**Comparison of the Protonations of 1 and 2 with Those Involving Other Pentadienyl-Metal-Phosphine Complexes.** It is interesting to compare the protonations of 1 and 2 with those of the related group 7 complexes, ($\eta^5$-pentadienyl)Mn[$(Me_2PCH_2)_3CMe$][1j] and ($\eta^5$-2,4-dimethylpentadienyl)Re($PMe_2Ph$)$_3$,[1j] which we reported earlier. The ground state of the protonated manganese product exhibits an agostic C-H-M interaction, while the protonated rhenium product contains a terminal hydride ligand, as shown.

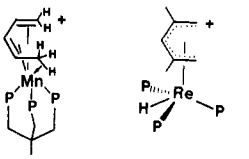


However, both ($C_5H_7$-$\mu$-H)Mn[$(Me_2PCH_2)_3CMe$]$^+$ and ($\eta^5$-2,4-dimethylpentadienyl)Re($PMe_2Ph$)$_3$(H)$^+$ undergo dynamic processes in solution, which involve reversible migration of the hydride ligand between the metal center and the termini of the pentadienyl ligand.[1j]

## Experimental Section

**General Data.** All manipulations were carried out under an inert atmosphere, using either drybox or Schlenk techniques. Diethyl ether, tetrahydrofuran, benzene, and durene were dried

(14) To our knowledge, these are the first examples of ($\eta^6$-arene)Rh($PEt_3$)$_2^+$ or ($\eta^6$-arene)Rh($PMe_3$)$_2^+$ complexes. Several synthetic approaches to ($\eta^6$-arene)Rh[$P(OPh)_3$]$_2^+$ have been reported. (a) Schrock, R. R.; Osborn, J. A. *J. Am. Chem. Soc.* **1971**, *93*, 3089. (b) Uson, R.; Lahuerta, P.; Reyes, J.; Oro, L. A. *Transition Met. Chem. (Weinheim, Ger.)* **1979**, *4*, 332. (c) Uson, R.; Lahuerta, P.; Reyes, J.; Oro, L. A.; Foces-Foces, C.; Cano, F. H.; Garcia-Blanco, S. *Inorg. Chim. Acta* **1980**, *42*, 75.

(15) The electronic origin of this effect is described in the following paper: Muetterties, E. L.; Bleeke, J. R.; Wucherer, E. J.; Albright, T. A. *Chem. Rev.* **1982**, *82*, 499.

with sodium/benzophenone and distilled before use. Pentane was dried over calcium hydride and distilled. Acetone was dried over potassium carbonate and distilled. $HBF_4{\cdot}OEt_2$ (Aldrich), $CH_3{}^+O_3SCF_3{}^-$ (Aldrich), $Ag^+O_3SCF_3{}^-$ (Aldrich), $(Ph_3P)_2N^+Cl^-$ (Aldrich), and $PMe_3$ (Strem) were all used without further purification. ($\eta^3$-2,4-Dimethylpentadienyl)$Rh(PEt_3)_2$ (1) and ($\eta^3$-2,4-dimethylpentadienyl)$Rh(PMe_3)_2$ (2) were synthesized by the literature procedure.[1h]

NMR experiments were performed on a Varian XL-300 NMR spectrometer. $^1H$ (300 MHz) and $^{13}C$ (75 MHz) spectra were referenced to tetramethylsilane. $^{31}P$ spectra (121 MHz) were referenced to $H_3PO_4$. In general, $^{13}C$ NMR peak assignments were made from gated-decoupled spectra. $^1H$ NMR peak assignments were then obtained from $^{13}C$–$^1H$ shift-correlated (HETCOR) 2D spectra. Some connectivities were ascertained from $^1H$–$^1H$ shift-correlated (COSY) 2D spectra. Infrared spectra were recorded on a Perkin-Elmer 283B spectrophotometer. Microanalyses were performed by Galbraith Laboratories, Inc., Knoxville, TN.

**Synthesis of ($\eta^5$-2,4-Dimethylpentadienyl)$Rh(PEt_3)_2(CH_3)^+O_3SCF_3{}^-$ (3). 1. Methylation of 1.** $CH_3{}^+O_3SCF_3{}^-$ (0.14 g, 0.85 mmol) in 5 mL of diethyl ether at −30 °C was added with swirling to a solution of 1 (0.37 g, 0.85 mmol) in 5 mL of diethyl ether at −30 °C. Dark red oily droplets separated immediately from the diethyl ether solution. After the diethyl ether solvent was removed under vacuum, the oily residue was dissolved in THF and cooled to −30 °C, causing **3** to crystallize as yellow flakes or blocks. Total yield: 0.48 g (94%). Yield of crystalline product: 0.35 g (69%).

**2. Reaction of ($\eta^3$-2,4-Dimethylpentadienyl)$Rh(PEt_3)_2(Me)(Cl)$ (5) with $Ag^+O_3SCF_3{}^-$.** To a solution of ($\eta^3$-2,4-dimethylpentadienyl)$Rh(PEt_3)_2(Me)(Cl)$ (**5**) (0.41 g, 0.85 mmol) in minimal tetrahydrofuran was added $Ag^+O_3SCF_3{}^-$ (0.22 g, 0.86 mmol) with stirring. The resulting solution was filtered to remove $Ag^+Cl^-$ and then evacuated to dryness. The residue was extracted with tetrahydrofuran and cooled to −30 °C, producing yellow, crystalline **3** (0.50 g, 0.84 mmol) (98% total yield). Anal. Calcd for $C_{21}H_{44}P_2RhO_3SF_3$: C, 42.14; H, 7.42; P, 10.35. Found: C, 42.21; H, 7.59; P, 10.12. $^1H$ NMR (20 °C, $(CD_3)_2CO$): $\delta$ 6.11 (d, $J$ = 3.7 Hz, 1, H(3)), 4.06 (s, 1, $H(1)_{syn}$), 2.69 (t, 1, $H(5)_{syn}$), 2.61 (s, 1, $H(1)_{anti}$), 2.22 (s, 3, H(6)'s), 2.20 (sextet, $J$ = 7.9 Hz, 3, phosphine $CH_2$'s), 2.10 (sextet, $J$ = 7.9 Hz, 3, phosphine $CH_2$'s), 1.94 (sextet, $J$ = 7.7 Hz, 3, phosphine $CH_2$'s), 1.93 (s, 3, H(7)'s), 1.66 (quintet of d, $J$ = 7.7, 4.9 Hz, 3, phosphine $CH_2$'s), 1.46 (d, $J$ = 8.6 Hz, 1, $H(5)_{anti}$), 1.16 (d of t, $J$ = 15.9, 7.9 Hz, 9, phosphine $CH_3$'s), 1.08 (d of t, $J$ = 15.0, 7.7 Hz, 9, phosphine $CH_3$'s), 0.29 (t of d, $J_{H-P}$ = 5.7 Hz, $J_{H-Rh}$ = 2.8 Hz, 3, H(8)'s). $^{13}C\{^1H\}$ NMR (20 °C, $(CD_3)_2CO$): $\eta$ 130.5 (s, C(2)), 125.4 (d, $J$ = 3.7 Hz, C(4)), 93.8 (d, $J$ = 15.6 Hz, C(3)), 74.6 (s, C(1)), 58.6 (d of d, $J$ = 36.6, 6.0 Hz, C(5)), 26.5, 22.9 (s's, C(6) and C(7)), 21.1 (d, $J_{C-P}$ = 28.4 Hz, phosphine $CH_2$'s), 18.5 (d, $J_{C-P}$ = 22.9 Hz, phosphine $CH_2$'s), 9.2 (d, $J_{C-P}$ = 5.3 Hz, phosphine $CH_3$'s), 8.4 (d, $J_{C-P}$ = 3.4 Hz, phosphine $CH_3$'s), 1.1 (t of d, $J_{C-P}$ = 13.6 Hz, $J_{C-Rh}$ = 7.3 Hz, C(8)). $^{31}P\{^1H\}$ NMR (20 °C, $(CD_3)_2CO$): $\delta$ 31.3 (d of d, $J_{P-Rh}$ = 150.3 Hz, $J_{P-P}$ = 22 Hz), 16.9 (d of d, $J_{P-Rh}$ = 129.2 Hz, $J_{P-P}$ = 22 Hz).

**Synthesis of ($\eta^5$-2,4-Dimethylpentadienyl)$Rh(PMe_3)_2(CH_3)^+O_3SCF_3{}^-$ (4). 1. Methylation of 2.** A procedure identical with method 1 for the synthesis of **3** (vida infra), except with 0.30 g (0.85 mmol) of **2**, produced 0.43 g of yellow **4** (99% yield).

**2. Reaction of ($\eta^3$-2,4-Dimethylpentadienyl)$Rh(PMe_3)_2(Me)(Cl)$ (6) with $Ag^+O_3SCF_3{}^-$.** A procedure identical with method 2 for the synthesis of **3** (vida infra), except with 0.34 g (0.85 mmol) of **6**, produced 0.42 g of **4** (96% yield). Anal. Calcd for $C_{15}H_{32}P_2RhO_3SF_3$: C, 35.02; H, 6.28. Found: C, 35.18; H, 6.26. $^1H$ NMR (20 °C, $(CD_3)_2CO$): $\delta$ 6.04 (d, $J$ = 4.6 Hz, 1, H(3)), 3.80 (s, 1, $H(1)_{syn}$), 2.70 (s, 1, $H(5)_{syn}$), 2.63 (s, 1, $H(1)_{anti}$), 2.32 (s, 3, H(6)), 1.95 (s, 3, H(7)), 1.83 (d of d, $J$ = 10.4, 1.0 Hz, 9, phosphine $CH_3$'s), 1.55 (d, $J$ = 9.8 Hz, 1, $H(5)_{anti}$), 1.47 (d of d, $J$ = 9.3, 0.8 Hz, 9, phosphine $CH_3$'s), 0.27 (d of d of d, $J$ = 7.1, 5.0, 2.1 Hz, 3, H(8)). $^{13}C\{^1H\}$ NMR (20 °C, $(CD_3)_2CO$): $\delta$ 129.0 (s, C(2)), 126.8 (s, C(4)), 94.0 (d, $J$ = 16.4 Hz, C(3)), 71.9 (s, C(1)), 60.9 (d, $J$ = 37.7 Hz, C(5)), 26.9 (s, C(6)), 23.0 (s, C(7)), 20.0 (d of d, $J$ = 35.0, 5.7 Hz, phosphine $CH_3$'s), 16.8 (d of d, $J$ = 29.7, 5.1 Hz, phosphine $CH_3$'s), 3.1 (d of t, $J$ = 20.6, 8.0 Hz, C(8)). $^{31}P\{^1H\}$ NMR (20 °C, $(CD_3)_2CO$): $\delta$ 7.5 (d of d, $J$ = 150.0, 29.9 Hz, P(1)), −0.2 (d of d, $J$ = 131.0, 29.9 Hz, P(2)).

**Reaction of 3 with $(Ph_3P)_2N^+Cl^-$. Synthesis of ($\eta^3$-2,4-Dimethylpentadienyl)$Rh(PEt_3)_2(Me)(Cl)$ (5).** $(Ph_3P)_2N^+Cl^-$ (0.15 g, 0.26 mmol) was added with stirring to a solution of **3** (0.16 g, 0.26 mmol) in 5 mL of tetrahydrofuran at −30 °C, causing the color of the solution to change from red to yellow. Pentane (20 mL) was added to precipitate white $(Ph_3P)_2N^+O_3SCF_3{}^-$. After filtration, the volatiles were removed under vacuum, leaving a yellow residue of **5**. **5** was extracted into pentane and, upon cooling to −30 °C, crystallized as yellow blocks. Total yield: 0.10 g (80%). Yield of crystalline product: 0.09 g (70%). Anal. Calcd for $C_{20}H_{44}P_2RhCl$: C, 49.53; H, 9.16. Found: C, 49.55; H, 9.20.

The following are very slow-exchange spectra for **5**. $^1H$ NMR (−20 °C, $(CD_3)_2CO$): $\delta$ 5.09 (s, 1, H(5)), 4.88 (s, 1, H(5)), 4.43 (d, $J_{H-P}$ = 8.7 Hz, 1, H(3)), 3.15 (d, $J_{H-P}$ = 4.3 Hz, 1, $H(1)_{syn}$), 2.94 (d, $J_{H-P}$ = 8.7 Hz, 1, $H(1)_{anti}$), 1.96 (m, $J$ = 7.3 Hz, 12, phosphine $CH_2$'s), 1.95 (s, 3, H(6)'s), 1.75 (s, 3, H(7)'s), 1.12 (d of t, $J_{H-P}$ = 13.1 Hz, $J_{H-H}$ = 7.3 Hz, 9, phosphine $CH_3$'s), 1.08 (d of t, $J_{H-P}$ = 12.7 Hz, $J_{H-H}$ = 7.3 Hz, 9, phosphine $CH_3$'s), −0.26 (t, $J_{H-P}$ = 5.2 Hz, 3, H(8)'s). $^{13}C\{^1H\}$ NMR (−20 °C, $(CD_3)_2CO$): $\delta$ 145.9 (s, C(4)), 125.0 (s, C(2)), 113.7 (s, C(5)), 84.3 (d, $J$ = 29.5 Hz, C(3)), 55.2 (d, $J$ = 31.1 Hz, C(1)), 25.8 (s, C(6)), 20.1 (s, C(7)), 18.4 (d, $J_{C-P}$ = 24.2 Hz, phosphine $CH_2$'s), 16.5 (d, $J_{C-P}$ = 21.4 Hz, phosphine $CH_2$'s), 8.9 (d, $J_{C-P}$ = 3.6 Hz, phosphine $CH_2$'s), 8.6 (d, $J_{C-P}$ = 4.5 Hz, phosphine $CH_3$'s), −7.4 (d of t, $J_{C-Rh}$ = 22.5 Hz, $J_{C-P}$ = 7.8 Hz, C(8)). $^{31}P\{^1H\}$ NMR (−20 °C, $(CD_3)_2CO$): $\delta$ 27.0 (d of d, $J_{P-Rh}$ = 153.3 Hz, $J_{P-P}$ = 8.2 Hz), 8.3 (d of d, $J_{P-Rh}$ = 136.8 Hz, $J_{P-P}$ = 8.2 Hz).

The following are fast-exchange spectra for **5**. $^1H$ NMR (50 °C, $(CD_3)_2CO$): $\delta$ 5.11 (s, 1, H(5)), 4.94 (s, 1, H(5)), 4.52 (t, $J$ = 4.5 Hz, 1, H(3)), 3.09 (t, $J$ = 3.0 Hz, 2, H(1)'s), 2.00 (quintet, $J$ = 7.6 Hz, 12, phosphine $CH_2$'s), 1.98 (s, 3, H(6)'s), 1.80 (s, 3, H(7)'s), 1.15 (d of t, $J_{H-P}$ = 13.5 Hz, $J_{H-H}$ = 7.6 Hz, 18, phosphine $CH_3$'s), −0.18 (t of d, $J_{H-P}$ = 5.6 Hz, $J_{H-Rh}$ = 1.9 Hz, 3, H(8)'s). $^{13}C\{^1H\}$ NMR (20 °C, $(CD_3)_2CO$): $\delta$ 146.0 (s, C(4)), 125.4 (C(2)), 113.4 (C(5)), 84.9 (t, $J_{C-P}$ = 16.2 Hz, C(3)), 55.3 (t, $J_{C-P}$ = 14.1 Hz, C(1)), 25.7 (s, C(6)), 19.9 (s, C(7)), 17.5 (br s, phosphine $CH_2$'s), 8.7 (s, phosphine $CH_3$'s), −7.4 (d, $J_{C-Rh}$ = 23.1 Hz, C(8)). The $^{31}P\{^1H\}$ NMR signals are broad at 50 °C; i.e., the fast-exchange limit has not been reached.

**Synthesis of ($\eta^3$-2,4-Dimethylpentadienyl)$Rh(PMe_3)_2(CH_3)(Cl)$ (6). 1. Reaction of 4 with $(Ph_3P)_2N^+Cl^-$.** A procedure identical with that described earlier for the synthesis of **5**, except with 0.13 g (0.26 mmol) of **4**, produced 0.80 g of yellow **6** (77% yield).

**2. Reaction of 5 with $PMe_3$.** $PMe_3$ (0.03 g, 0.29 mmol) was added to a solution of **5** (0.025 g, 0.052 mmol) in 0.5 mL of acetone. After quick removal of the volatiles under vacuum, the yellow residue was dissolved in pentane and cooled to −30 °C, causing **6** to crystallize as yellow blocks. Yield: 0.020 g (96%). Anal. Calcd for $C_{14}H_{32}P_2RhCl$: C, 41.96; H, 8.06. Found: C, 41.63; H, 7.89. $^1H$ NMR (20 °C, $(CD_3)_2CO$): $\delta$ 5.02 (s, 1, H(5)), 4.90 (s, 1, H(5)), 4.28 (d, $J_{H-P}$ = 8.9 Hz, 1, H(3)), 2.97 (d, $J_{H-P}$ = 9.3 Hz, 1, $H(1)_{syn}$), 2.93 (dd, $J$ = 5.2 Hz, 2.7 Hz, 1, $H(1)_{anti}$), 1.94 (s, 3, H(6)'s), 1.76 (s, 3, H(7)'s), 1.51 (d, $J_{H-P}$ = 10.5 Hz, 9, phosphine $CH_3$'s), 1.44 (d, $J_{H-P}$ = 8.7 Hz, 9, phosphine $CH_3$'s), −0.30 (t of d, $J_{H-P}$ = 6.4 Hz, $J_{H-Rh}$ = 2.2 Hz, 3, H(8)'s). $^{13}C\{^1H\}$ NMR (20 °C, $(CD_3)_2CO$): $\delta$ 146.73 (s, C(4)), 125.7 (s, C(2)), 112.9 (s, C(5)), 81.9 (d, $J_{C-P}$ = 32.5 Hz, C(3)), 57.6 (d, $J_{C-P}$ = 32.4 Hz, C(1)), 25.8 (s, C(6)), 19.7 (s, C(7)), 17.8 (d, $J_{C-P}$ = 27.8 Hz, phosphine $CH_3$'s), 15.2 (d, $J_{C-P}$ = 26.4 Hz, phosphine $CH_3$'s), −3.7 (d of t, $J_{C-Rh}$ = 23.5 Hz, $J_{C-P}$ = 7.2 Hz, C(8)). $^{31}P\{^1H\}$ NMR (20 °C, $(CD_3)_2CO$): $\delta$ 5.3 (d of d, $J_{P-Rh}$ = 151.8 Hz, $J_{P-P}$ = 10.9 Hz), −7.8 (d of d, $J_{P-Rh}$ = 140.1 Hz, $J_{P-P}$ = 10.9 Hz).

**Protonation of ($\eta^3$-2,4-Dimethylpentadienyl)$Rh(PEt_3)_2$ (1). Synthesis of ($\eta^4$-2,4-Dimethylpentadiene)$Rh(PEt_3)_2{}^+BF_4{}^-$ (7).** $HBF_4{\cdot}OEt_2$ (0.12 g, 0.74 mmol) in 5 mL tetrahydrofuran at −30 °C was added with swirling to a solution of **1** (0.32 g, 0.74 mmol) in 5 mL of tetrahydrofuran at −30 °C, causing the color of the solution to change immediately from red-orange to red-purple. Attempts to isolate solid **7** from this solution led to loss of 2,4-dimethylpentadiene and decomposition. However, **7** can be stored for a short time in tetrahydrofuran at −30 °C and used in situ. $^1H$ NMR (−40 °C, $CD_2Cl_2$): $\delta$ 4.76 (s, 1, H(3)), 3.56 (s, 1, $H(1)_{syn}$), 2.66 (s, 1, $H(1)_{anti}$), 1.95 (s, 3, H(6)'s), 1.71 (br s, 12, phosphine $CH_2$'s), 1.60 (s, 3, H(7)'s), 1.15 (s, 3, H(5)'s), 0.99 (m, 18, phosphine $CH_3$'s). $^{13}C\{^1H\}$ NMR (−80 °C, $CD_2Cl_2$): $\delta$ 116.0 (d, $J$ = 6.3 Hz,

**Table VII. Crystal and Diffraction Data for 3, 5, and 9**

| | 3 | 5 | 9 |
|---|---|---|---|
| formula | $C_{21}H_{44}F_3O_3P_2RhS$ | $C_{20}H_{44}ClP_2Rh$ | $C_{22}H_{44}BF_4P_2Rh$ |
| mol wt | 598.49 | 484.88 | 560.25 |
| space group | $P2_1/c$ | $P2_1/c$ | $P2_1/n$ |
| $a$, Å | 11.310 (2) | 12.962 (3) | 8.349 (2) |
| $b$, Å | 13.507 (7) | 8.236 (2) | 10.843 (8) |
| $c$, Å | 18.226 (3) | 22.758 (6) | 29.535 (9) |
| $\beta$, deg | 95.97 (2) | 94.19 (2) | 91.96 (2) |
| $V$, Å$^3$ | 2769 (3) | 2423 (2) | 2672 (3) |
| $Z$ | 4 | 4 | 4 |
| cryst color | yellow | yellow | red |
| cryst dimens, mm | 0.2 × 0.3 × 0.6 | 0.4 × 0.3 × 0.3 | 0.6 × 0.15 × 0.15 |
| $d_{calcd}$, g/cm$^3$ | 1.436 | 1.329 | 1.392 |
| radiatn, Å | Mo K$\alpha$, $\lambda$ = 0.71069 | Mo K$\alpha$, $\lambda$ = 0.71069 | Mo K$\alpha$, $\lambda$ = 0.71069 |
| $\mu$, cm$^{-1}$ | 8.310 | 9.362 | 7.807 |
| abs corr | none | psi scans | psi scans |
| max, min, av trans factors | | 0.9993, 0.8953, 0.9565 | 0.9969, 0.8080, 0.8712 |
| scan type | $\omega$ | $\theta$–$2\theta$ | $\theta$–$2\theta$ |
| scan rate, deg/min | variable, 2–29 | variable, 4–29 | variable, 4–29 |
| $2\theta$ min, deg | 3.0 | 3.0 | 3.0 |
| $2\theta$ max, deg | 60.0 | 45.0 | 55.0 |
| octants collected | $h,k,\pm l$ | $h,k,\pm l$ | $h,k,\pm l$ |
| no. of reflcts measd | 8345 | 3378 | 5379 |
| no. of reflcts with $I > 3\sigma(I)$ | 3986 | 2624 | 3563 |
| no. of parameters varied | 280 | 329 | 246 |
| data/parameter ratio | 14.2 | 8.0 | 14.5 |
| final $R_F$[a] | 0.050 | 0.033 | 0.083 |
| final $R_{wF}$[b] | 0.066 | 0.047 | 0.124 |

[a] $R_F = \sum||F_o| - |F_c||/\sum|F_o|$. [b] $R_{wF} = [\sum w(|F_o| - |F_c|)^2/\sum w|F_o|^2]^{1/2}$; $w = 1/\sigma(|F_o|)$.

C(2) or C(4)), 109.0 (d, $J$ = 6.1 Hz, C(2) or C(4)), 97.9 (d, $J$ = 14.8 Hz, C(3)), 64.4 (d of d, $J$ = 19.0 Hz, 3.8 Hz, C(1)), 33.5 (s, C(7)), 28.0 (s, C(5)), 25.8 (s, C(6)), 17.9 (d, $J_{C-P}$ = 27.2 Hz, phosphine $CH_2$'s), 16.8 (d, $J_{C-P}$ = 25.2 Hz, phosphine $CH_2$'s), 8.1 (s, phosphine $CH_3$'s). $^{31}P\{^1H\}$ NMR (−80 °C, $CD_2Cl_2$): $\delta$ 23.8 (d of d, $J_{P-Rh}$ = 180 Hz, $J_{P-P}$ = 43 Hz), 22.6 (d of d, $J_{P-Rh}$ = 176 Hz, $J_{P-P}$ = 43 Hz).

**Conversion of 7 to ($\eta^6$-Benzene)Rh($PEt_3$)$_2^+BF_4^-$ (8).** Benzene (0.078 g, 1.0 mmol) was added to a solution of **7** (0.20 g, 0.39 mmol) in 10 mL of tetrahydrofuran, causing the color of the solution to change immediately from red-purple to red-orange. Evacuation of the volatiles left **8** as a yellow solid. Yield: 0.20 g (100%). Anal. Calcd for $C_{18}H_{36}P_2RhBF_4$: C, 42.88; H, 7.21. Found: C, 42.73; H, 7.03. $^1H$ NMR (20 °C, $(CD_3)_2CO$): $\delta$ 6.76 (s, 6, benzene CH's), 1.54 (m, 12, phosphine $CH_2$'s), 1.20 (m, 18, phosphine $CH_3$'s). $^{13}C\{^1H\}$ NMR (20 °C, $(CD_3)_2CO$): $\delta$ 100.8 (s, benzene CH's), 17.8 (virtual t, $J_{C-P}$ = 28.9 Hz, phosphine $CH_2$'s), 8.6 (s, phosphine $CH_3$'s). $^{31}P\{^1H\}$ NMR (20 °C, $(CD_3)_2CO$): $\delta$ 41.2 (d, $J_{P-Rh}$ = 199 Hz).

**Conversion of 7 to ($\eta^6$-Durene)Rh($PEt_3$)$_2^+BF_4^-$ (9).** Durene (0.053 g, 0.39 mmol) was added to a solution of **7** (0.20 g, 0.39 mmol) in 10 mL of tetrahydrofuran, causing the color to change gradually from red-purple to red. Evacuation of the volatiles left **9** as a red-brown solid. Yield: 0.21 g (100%). Anal. Calcd for $C_{22}H_{44}P_2RhBF_4$: C, 47.16; H, 7.93. Found: C, 46.76; H, 8.12. $^1H$ NMR (17 °C, $CD_2Cl_2$): $\delta$ 5.36 (s, 2, durene CH's), 2.35 (s, 12, durene $CH_3$'s), 1.54 (quintet, $J$ = 8 Hz, 12, phosphine $CH_2$'s), 0.99 (d of t, $J$ = 16 Hz, 8 Hz, 18, phosphine $CH_3$'s). $^{13}C\{^1H\}$ NMR (17 °C, $CD_2Cl_2$): $\delta$ 117.2 (durene C's), 97.9 (durene CH's), 20.5 (virtual t, $J_{C-P}$ = 30.7 Hz, phosphine $CH_2$'s), 19.0 (durene $CH_3$'s), 8.2 (phosphine $CH_3$'s). $^{31}P\{^1H\}$ NMR (17 °C, $CD_2Cl_2$): $\delta$ 33.8 (d, $J_{P-Rh}$ = 199 Hz).

**Protonation of ($\eta^3$-2,4-Dimethylpentadienyl)Rh($PMe_3$))$_2$ (2). Synthesis of ($\eta^5$-2,4-Dimethylpentadienyl)Rh($PMe_3$)$_2H^+BF_4^-$ (10) and ($\eta^4$-2,4-Dimethylpentadiene)Rh($PMe_3$)$_2^+BF_4^-$ (11).** $HBF_4$·$OEt_2$ (0.092 g, 0.57 mmol) in 5 mL of tetrahydrofuran at −30 °C was added with swirling to a solution of **2** (0.20 g, 0.57 mmol) in 5 mL of tetrahydrofuran at −30 °C, causing the color of the solution to change immediately from red-orange to red-purple. Attempts to isolate solid **10** and **11** from this solution led to loss of 2,4-dimethylpentadiene and decomposition. However, the equilibrium mixture of **10** (30%) and **11** (70%) can be stored for a short time in tetrahydrofuran at −30 °C and used in situ.

**NMR Spectra for 10.** $^1H$ NMR (−35 °C, $CD_2Cl_2$): $\delta$ 5.72 (s, 1, H(3)), 3.65 (s, 1, $H(1)_{syn}$), 3.14 (s, 1, $H(5)_{syn}$), 2.17 (s, 3, H(6)'s), 1.76 (d, $J$ = 8.9 Hz, 9, phosphine $CH_3$'s), 1.39 (s, 3, H(7)'s), −14.61 (m, 1, Rh–H). (Signals due to $H(1)_{anti}$, $H(5)_{anti}$, and one $PMe_3$ ligand are obscured.) $^{13}C\{^1H\}$ NMR (−35 °C, $CD_2Cl_2$): $\delta$ 125.0 (C(2)), 123.3 (C(4)), 93.1 (d, $J$ = 12.0 Hz, C(3)), 70.8 (C(1)), 56.6 (d of d, $J$ = 32.4, 7.5 Hz, C(5)), 27.9 (C(6))), 26.6 (C(7)), 22.6 (d, $J_{C-P}$ = 34.3 Hz, phosphine $CH_3$'s), 20.5 (d, $J_{C-P}$ = 29.8 Hz, phosphine $CH_3$'s). $^{31}P\{^1H\}$ NMR (−35 °C, $CD_2Cl_2$): $\delta$ 2.4 (d of t, $J_{P-Rh}$ = 143 Hz, $J_{P-P} \approx J_{P-H}$ = 22 Hz, P(1)), −9.3 (d of d of d, $J_{P-Rh}$ = 126 Hz, $J_{P-P}$ = 22 Hz, $J_{P-H}$ = 11 Hz, P(2)).

**NMR Spectra for 11.** $^1H$ NMR (−35 °C, $CD_2Cl_2$): $\delta$ 4.77 (s, 1, H(3)), 3.59 (s, 1, $H(1)_{syn}$), 2.68 (s, 1, $H(1)_{anti}$), 2.02 (s, 3, H(6)'s), 1.63 (s, 3, H(7)'s), 1.54 (d, $J$ = 9.7 Hz, 9, phosphine $CH_3$'s), 1.44 (d, $J$ = 10.4 Hz, 9, phosphine $CH_3$'s), 1.09 (s, 3, H(5)'s). $^{13}C\{^1H\}$ NMR (−35 °C, $CD_2Cl_2$): $\delta$ 118.6 (C(2) or C(4)), 103.1 (C(2) or C(4)), 96.2 (C(3)), 63.6 (d, $J$ = 14.7 Hz, C(1)), 33.0 (C(7)), 27.8 (C(5)), 26.2 (C(6)), 19.3 (d, $J_{C-P}$ = 28.4 Hz, phosphine $CH_3$'s), 18.1 (d, $J_{C-P}$ = 28.2 Hz, phosphine $CH_3$'s). $^{31}P\{^1H\}$ NMR (−35 °C, $CD_2Cl_2$): $\delta$ −12.9 (d of d, $J_{P-Rh}$ = 170 Hz, $J_{P-P}$ = 50 Hz, P(1)), −16.1 (d of d, $J_{P-Rh}$ = 182 Hz, $J_{P-P}$ = 50 Hz, P(2)).

**Conversion of 10/11 to ($\eta^6$-Benzene)Rh($PMe_3$)$_2^+BF_4^-$ (12).** A procedure identical with that described earlier for the synthesis of **8**, except with 0.17 g (0.39 mmol) of **10**/**11**, produced 0.11 g of yellow **12** (70% yield). Anal. Calcd for $C_{12}H_{24}RhP_2BF_4$: C, 34.31; H, 5.77. Found: C, 33.91; H, 5.23. $^1H$ NMR (−35 °C, $CD_2Cl_2$): $\delta$ 6.42 (s, 6, benzene CH's), 1.7 (m, 18, phosphine $CH_3$'s). $^{13}C\{^1H\}$ NMR (−35 °C, $CD_2Cl_2$): $\delta$ 99.6 (benzene CH's), 15.4 (virtual t, $J_{C-P}$ = 39.7 Hz, phosphine $CH_3$'s). $^{31}P\{^1H\}$ NMR (−35 °C, $CD_2Cl_2$): $\delta$ −5.0 (d, $J_{P-Rh}$ = 199 Hz).

**Conversion of 10/11 to ($\eta^6$-Durene)Rh($PMe_3$)$_2^+BF_4^-$ (13).** A procedure identical with that described earlier for the synthesis of **9**, except with 0.17 g (0.39 mmol) of **10**/**11**, produced 0.13 g of red-brown **13** (70% yield). Anal. Calcd for $C_{16}H_{32}P_2RhBF_4$: C, 40.36; H, 6.79. Found: C, 40.08; H, 6.56. $^1H$ NMR (18 °C, $CD_2Cl_2$): $\delta$ 5.42 (s, 2, durene CH's), 2.33 (s, 12, durene $CH_3$'s), 1.44 (virtual m, 18, phosphine $CH_3$'s). $^{13}C\{^1H\}$ NMR (18 °C, $CD_2Cl_2$): 116.7 (durene C's), 98.4 (durene CH's), 22.0 (virtual t, $J_{C-P}$ = 34.5 Hz, phosphine $CH_3$'s), 18.7 (durene $CH_3$'s). $^{13}P\{^1H\}$ NMR (18 °C, $CD_2Cl_2$): $\delta$ −1.8 (d, $J_{P-Rh}$ = 200 Hz).

**X-ray Diffraction Studies of 3 and 5.** Single crystals of **3**, **5**, and **9** were sealed in glass capillaries under an inert atmosphere. Data were collected at room temperature on a Nicolet P3 diffractometer, using graphite-monochromated Mo K$\alpha$ radiation. All data reduction and structure refinement were done by using the Enraf-Nonius structure determination package (modified by

B.A. Frenz and Assoc., Inc., College Station, TX) on a VAX 11/780 computer.[16] Crystal data and details of data collection and structure analysis are summarized in Table VII.

In each case, the structure was solved by standard Fourier techniques, following the location of the rhodium atom from a Patterson map. For **3**, all non-hydrogen atoms were refined anisotropically, while hydrogen atoms were added at idealized positions by using the program HYDRO and included in the structure factor calculations, but not refined. For **5**, all non-hydrogen atoms except for the carbons in one $PEt_3$ ethyl group (C(23)–C(23)′) were refined anisotropically. Atoms C(23) and C(23)′ each exhibited a twofold disorder, which we were able to model successfully by using a multiplicity of 0.5 for each site. Both sets of C(23) atoms (labeled C(23)A and C(23)B in Tables III and IV and C(23)′ atoms (labeled C(23)C and C(23)D) were refined isotropically. All hydrogen atoms except for those on the disordered ethyl group were located on difference Fourier maps. The positions of these hydrogen atoms (except for H(62)) were refined and were included in the structure factor calculations. For **9**, all non-hydrogen atoms except the boron and the four fluorines in the $BF_4^-$ group were refined anisotropically. The fluorine atoms exhibited very large isotropic thermal parameters consistent with a disorder problem. However, independent sets of fluorine atoms (in sites of partial occupancy) were not resolvable in the electron density maps. Therefore, a disorder could not be modeled, and the boron and four fluorine atoms were refined isotropically at full occupancy. All hydrogen atoms were added at idealized positions by using the program HYDRO and included in the structure factor calculations, but not refined.

**Solution Dynamics of Compounds 3 and 5.** Samples were dissolved in $(CD_3)_2CO$ or $C_2D_4Cl_2$, and NMR spectra were recorded over the temperature range −80 to 80 °C. The exchange rate constant, $k_c$, at the coalescence temperature for each exchange process[17] was calculated by using the formula

$$k_c = \frac{\pi(\Delta\nu)}{2^{1/2}}$$

where $\Delta\nu$ is the difference in frequency between the two exchanging sites in the stopped exchange limit.[18] This exchange rate constant was then used to determine the free energy of activation, $\Delta G^\ddagger$, at the coalescence temperature, $T_c$, from the Eyring equation

$$k = \frac{k'}{\hbar} T e^{-\Delta G^\ddagger/RT}$$

where $k'$ = Boltzmann's constant, $\hbar$ = Planck's constant, and $R$ = ideal gas constant.[19]

## Summary

From this study, several salient features of the reactivity of $(\eta^3$-2,4-dimethylpentadienyl)$Rh(PR_3)_2$ complexes have emerged. First, the electron-rich metal center reacts readily with electrophiles such as $CH_3^+$ and $H^+$. These electrophilic additions are accompanied by shifts of the 2,4-dimethylpentadienyl ligands from the $\eta^3$-bonding mode to the $\eta^5$-bonding mode, generating 18e Rh(III) products.

Second, pentadienyl ligand shifts give rise to nucleophilic addition and substitution chemistry. For example, the nucleophilic additions of $Cl^-$ to $[(\eta^5$-2,4-dimethylpentadienyl)$Rh(PR_3)_2(Me)]^+$ complexes proceed via 16e intermediates, which are generated by $\eta^5 \rightarrow \eta^3$ pentadienyl ligand shifts. Similarly, $\eta^3 \rightarrow \eta^1 \rightarrow \eta^3$ ligand shifts are responsible for both the dynamic behavior and the nucleophilic substitution chemistry exhibited by $(\eta^3$-2,4-dimethylpentadienyl)$Rh(PEt_3)_2(Me)(Cl)$.

Third, the hydride ligands that result from protonation of $(\eta^3$-2,4-dimethylpentadienyl)$Rh(PR_3)_2$ complexes exhibit a high aptitude for migration to the termini of the 2,4-dimethylpentadienyl groups. The resulting $[(\eta^4$-2,4-dimethylpentadienyl)$Rh(PR_3)_2]^+$ complexes, when treated with arenes, lose 2,4-dimethylpentadiene and are converted to $[(\eta^6$-arene)$Rh(PR_3)_2]^+$ complexes. In contrast to hydride ligands, methyl ligands show no tendency to migrate.

**Acknowledgment.** Support from the National Science Foundation (Grant CHE-8520680) is gratefully acknowledged. Washington University's High Resolution NMR Facility was funded in part by National Institutes of Health Biomedical Research Support Instrument Grant 1 S10 RR02004 and by a gift from Monsanto Co.

**Registry No.** **1**, 104779-57-9; **2**, 104779-56-8; **3**, 114422-97-8; **4**, 114422-93-4; **5**, 114422-90-1; **6**, 114422-91-2; **7**, 114422-81-0; **8**, 114443-22-0; **9**, 114422-83-2; **10**, 114422-95-6; **11**, 114422-85-4; **12**, 114422-87-6; **13**, 114422-89-8; $CH_3^+O_3SCF_3^-$, 333-27-7; $Ag^+O_3SCF_3^-$, 2923-28-6; $(Ph_3P)_2N^+Cl^-$, 21050-13-5.

**Supplementary Material Available:** Listing of final atomic coordinates, thermal parameters, bond lengths, bond angles, torsional angles, and significant least-squares planes for **3**, **5**, and **9** and an ORTEP drawing of Rh–P(2) moiety of **5**, showing orientation of the disordered ethyl group, C(23)–C(23)′ (27 pages); listings of observed and calculated structure factor amplitudes (41 pages). Ordering information is given on any current masthead page.

(16) Atomic scattering factors were obtained from: *International Tables for X-Ray Crystallography*; Kynoch: Birmingham, England, 1974; Vol. IV.

(17) The coalescence of the $^{13}C$ NMR signals due to pentadienyl methyl carbons C(6) and C(7) was used to calculate the rotational barrier in **3**, while the coalescence of the $H(1)_{anti}$ and $H(1)_{syn}$ signals in **5** was used to calculate $\Delta G^\ddagger$ for the $\eta^3 \rightleftharpoons \eta^1 \rightleftharpoons \eta^3$ fluxional process.

(18) Pople, J. A.; Schneider, W. G.; Bernstein, H. J. *High Resolution Nuclear Magnetic Resonance*; McGraw-Hill: New York, 1959; p 223.

(19) Lowry, T. H.; Richardson, K. S. *Mechanism and Theory in Organic Chemistry*; Harper and Row: New York, 1976; p 194.